

## Electronic Supplementary Information for 'Water slowing down drives the occurrence of the low temperature dynamical transition in microgels'

Letizia Tavagnacco,<sup>1,2</sup> Marco Zanatta,<sup>3</sup> Elena Buratti,<sup>4</sup> Monica Bertoldo,<sup>4</sup> Ester Chiessi,<sup>5</sup>  
Markus Appel,<sup>6</sup> Francesca Natali,<sup>7</sup> Andrea Orecchini,<sup>8,9</sup> and Emanuela Zaccarelli<sup>1,2</sup>

<sup>1</sup> *CNR Institute of Complex Systems, Uos Sapienza, Piazzale Aldo Moro 2, 00185 Rome, Italy*

<sup>2</sup> *Department of Physics, Sapienza University of Rome, Piazzale Aldo Moro 2, 00185 Rome, Italy*

<sup>3</sup> *Department of Physics, University of Trento, via Sommarive 14, 38123 Trento, Italy*

<sup>4</sup> *Department of Chemical, Pharmaceutical and Agricultural Sciences,  
University of Ferrara, Via L. Borsari 46, 44121 Ferrara, Italy*

<sup>5</sup> *Department of Chemical Science and Technologies,  
University of Rome Tor Vergata, Via della Ricerca Scientifica I, 00133 Rome, Italy*

<sup>6</sup> *Institut Laue-Langevin, 71 avenue des Martyrs, CS 20156, 38042 GRENOBLE Cedex 9, France*

<sup>7</sup> *CNR-IOM, Operative Group Grenoble (OGG), Institut Laue Langevin, F-38042 Grenoble, France*

<sup>8</sup> *Dipartimento di Fisica e Geologia, Università di Perugia, Via Alessandro Pascoli, 06123 Perugia, Italy*

<sup>9</sup> *CNR-IOM c/o Dipartimento di Fisica e Geologia,  
Università di Perugia, Via Alessandro Pascoli, 06123 Perugia, Italy*

### DETAILS ON MATERIALS AND MICROGEL SYNTHESIS

*N*-isopropylacrylamide (NIPAM) (Sigma-Aldrich, St. Louis, MO, USA), purity 97%, and deuterated *N*-isopropylacrylamide (d-10) (d-NIPAM) (Polymer Source, Inc, Quebec, Canada), purity  $\geq 98\%$ , were purified through recrystallized from hexane, dried under reduced pressure (0.01 mmHg) at room temperature and stored at 253 K. *N,N'*-methylenebisacrylamide (BIS) (Sigma-Aldrich, St. Louis, MO, USA), electrophoresis grade, was purified through recrystallization from methanol, dried under reduced pressure (0.01 mmHg) at room temperature and stored at 253 K. Sodium dodecyl sulphate (SDS) (Sigma-Aldrich, St. Louis, MO, USA), purity 98%, and potassium persulfate (KPS) (Sigma-Aldrich, St. Louis, MO, USA), purity 98%, were used as received. Ultrapure water (resistivity: 18.2 MW/cm at room temperature) was obtained with Arium<sup>®</sup> pro Ultrapure water purification Systems, Sartorius Stedim. All other solvents (Sigma Aldrich RP grade) were used as received. Dialysis membrane, SpectraPor<sup>®</sup> 1, MWCO 6-8 kDa (Spectrum Laboratories, Inc., Piscataway, NJ, USA) was soaked in distilled water for 2 h and then thoroughly rinsed before use.

Two microgels, a protiated one and a deuterated one, were synthesized with the same procedure but with different monomers, NIPAM and d-NIPAM, respectively.

For the synthesis of the protiated microgel, NIPAM (0.137 M) was solubilized in 1560 mL of ultrapure water in a 2 L four-neck jacketed reactor in presence of BIS (1.87 mM) as crosslinker and SDS (7.82 mM) as surfactant. After deoxygenation by bubbling nitrogen for 1 h, the solution was heated at 343 K and the initiator KPS (2.44 mM, previously dissolved in 10 mL of deoxygenated water) was added to start the polymerization, carried out for 4 hours. The final dispersion was purified by dialysis (MWCO 6–8 kDa) for 2 weeks with several changes of distilled water and then concentrated by lyophilisation up to 10 wt % in  $H_2O$ . PNIPAM dispersion in  $D_2O$  was prepared by two cycles of lyophilisation to dryness and re-dispersion in deuterium oxide (10 wt %) to avoid  $H_2O$  contamination of the samples.

The synthesis of the deuterated microgel was carried out in a 250 mL four-neck jacketed reactor by replacing NIPAM with an equimolar amount of d-NIPAM, dissolved in 125 mL of ultrapure water, and keeping the concentrations of all the other reactants the same. The purification of the dispersion and the concentration by lyophilization up to 10 wt % in  $H_2O$  was carried out in a similar manner to the protiated microgel. For both microgels, non-deuterated BIS was used as crosslinker, by assuming its concentration negligible with respect to the monomer one.

Sample at 40, 50 and 60 wt % were prepared directly in the aluminium cells for the EINS experiments, by evaporation of the exceeding solvent of the dispersion at 10 wt % in dry atmosphere using a desiccator under moderate vacuum ( $\sim 10$  mmHg) and weighting the samples until the final concentrations was reached.

## DETAILS ON ELASTIC INCOHERENT NEUTRON SCATTERING EXPERIMENTS

Representative examples of the measured  $I(Q; 0)$  on IN16B for D-PNIPAM in  $H_2O$  at 60 wt % are shown in Fig. S1.

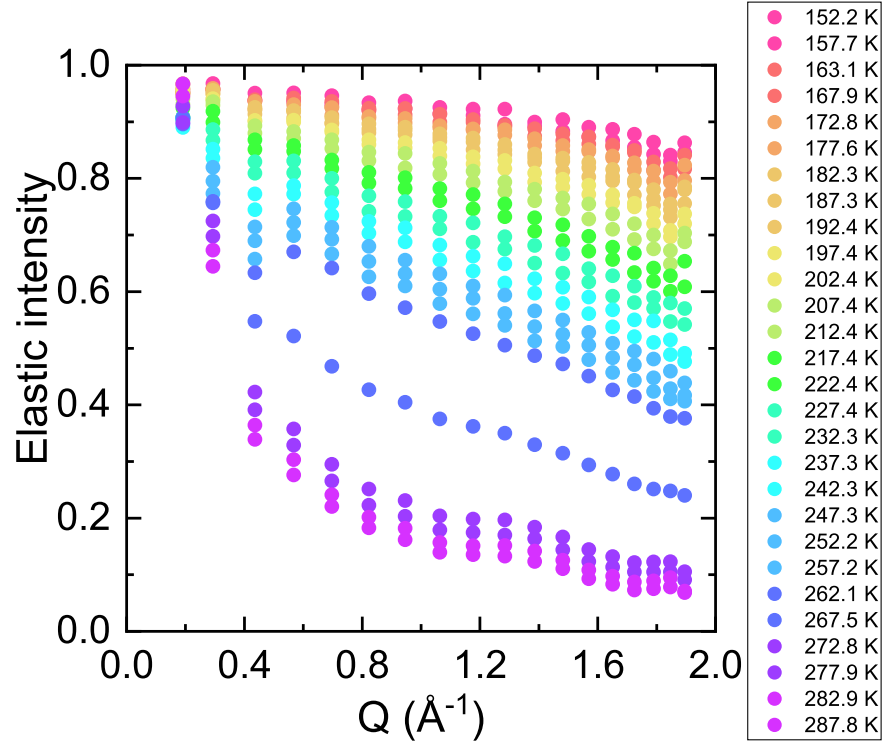


FIG. S1.  $I(Q; 0)$  measured on IN16B for D-PNIPAM in  $H_2O$  at 60 wt % as a function of temperature.

## DETAILS ON MOLECULAR DYNAMICS SIMULATIONS

All-atom molecular dynamics simulations of PNIPAM microgels suspensions at PNIPAM mass fractions of 40 and 60% (w/w) were performed following a similar procedure. For each system, equilibration was first carried out at 293 K in a pressure bath at 1 bar up to a constant density value, i.e. tot-drift lower than  $2 \times 10^{-3} \text{ g cm}^{-3}$  over 20 ns. A similar equilibration protocol was applied at each temperature explored. The leapfrog integration algorithm was employed with a time step of 2 fs. The length of bonds involving hydrogen atoms was kept fixed using the LINCS algorithm. Cubic periodic boundary conditions and minimum image convention were applied.

# WATER AND PNIPAM DYNAMICS FROM MOLECULAR DYNAMICS SIMULATIONS

To probe the occurrence of the low temperature dynamical transition in the numerical simulations of microgels, we first monitored the mean squared displacement (MSD). Fig. S2 shows the MSDs calculated for PNIPAM hydrogen atoms at the resolution time  $\tau=1800$  ps of IN16B for the simulations of PNIPAM network at a concentration 60 wt % and it compares them to the numerical and experimental MSDs reported in Ref. [S1] for PNIPAM linear chains in the same experimental conditions. The linear fitting representation, which is conventionally used for proteins, is also illustrated in Fig. S2. The linear representation appears compatible with the interpretation that a dynamical transition occurs for both linear chains and polymer network at  $T_d \sim 225$  K.

For completeness, Fig. S3 reports the time dependence of the MSDs calculated individually for water and PNIPAM in the simulations of PNIPAM 60 wt % as a function of temperature. We observe that for a large temperature range water can reach a diffusive regime, even at the resolution time of 1800 ps. Differently, within the entire explored time window, PNIPAM never reaches a diffusive regime.

TABLE S1. Comparison between the transition temperatures  $T_d$  and  $T_m$  obtained from EINS measurements on the spectrometer IN16B.

| Sample                     | $T_d$ (K)       | $T_m$ (K)       |
|----------------------------|-----------------|-----------------|
| D-PNIPAM in $H_2O$ 60 wt % | $209.0 \pm 0.6$ | $264.6 \pm 0.1$ |
| H-PNIPAM in $H_2O$ 60 wt % | $223.2 \pm 0.6$ | $264.4 \pm 0.6$ |
| H-PNIPAM in $D_2O$ 60 wt % | $227.7 \pm 0.8$ | $268.5 \pm 0.2$ |

$T_d$ ,  $T_m$ , and error bars were determined from the fit of the integrated elastic intensity as a function of temperature.

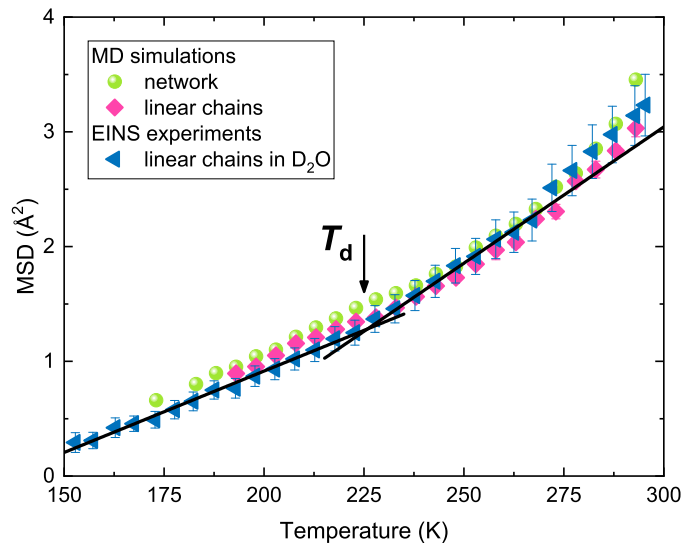


FIG. S2. Comparison between the numerical MSDs calculated at 1800 ps for the polymer hydrogen atoms in the simulations of PNIPAM network 60 wt% (green circles) with the numerical (pink diamonds) and experimental (blue triangles) reported at the same conditions for PNIPAM linear chains in ref [S1]. The transition temperature obtained by applying the conventional linear fitting procedure on the experimental data (black lines) is marked with an arrow. Error bars amount to one standard deviation and, when not visible, are within the symbol size.

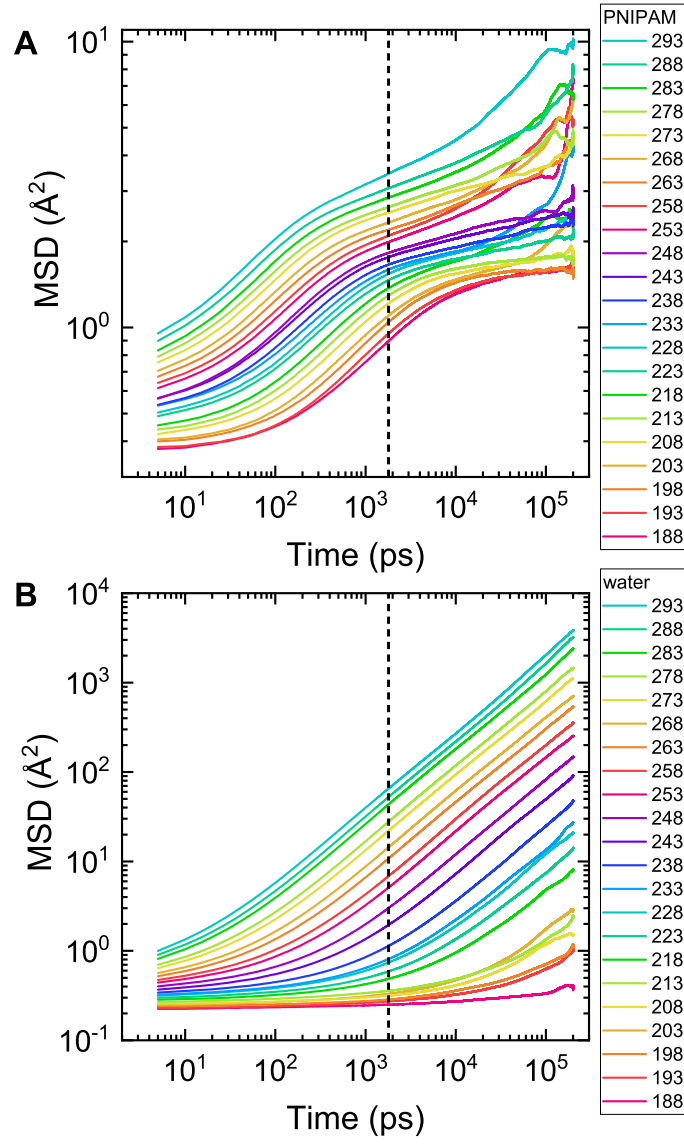


FIG. S3. Time evolution of the numerical mean squared displacement of hydrogen atoms as calculated for A) PNIPAM and B) water in the simulations of PNIPAM 60 wt %. Data are shown for the entire temperature range explored  $188 \text{ K} < T < 293 \text{ K}$ . The vertical dashed lines marks the MSD values at 1800 ps.

# CHARACTERIZATION OF MICROGELS NETWORK MESH SIZE

To characterize the structure of PNIPAM microgels and get information on the internal architecture, we have measured the form factor  $P(Q)$  by performing small angle neutron scattering experiments on protiated PNIPAM microgels in deuterated water at low polymer concentration  $\sim 1\%$  wt, as reported in Fig. S4 [S2]. To have an estimate of the mesh size of the polymer network we fitted the high- $Q$  decay of the form factor using the Lorentzian form [S3]:

$$P(q) \propto \frac{1}{[1 + \frac{D_f+1}{3}\xi^2 q^2]^{D_f/2}} \quad (\text{S1})$$

where  $D_f$  is the fractal dimension of the correlated domains and  $\xi$  is the length over which correlation fluctuations are spatially correlated. The resulting fitting parameters are  $D_f = 1.4$  and  $\xi = 100 \pm 20$ , the latter being the length over which correlation fluctuations are spatially correlated in the fuzzy corona of the microgels [S4]. We remark that this is a measurement of the larger domains existing in the microgel corona at very low polymer concentrations, we can expect that in the interior of the microgels at 60% wt, investigated in the present manuscript, the resulting mesh size will be even smaller than this value. Of course, these are difficult measurements, but a confirmation of this comes from the study of Houston et al [S5], where they measure the form factors of microgels in a sea of deuterated polymer chains and report a value of the mesh size which decreases with polymer concentration by roughly 30%. Hence we can expect that a realistic mesh size of the corona is of less than 10 nm, even smaller at the interior of the microgel. Such a heterogeneous environment can then be easily thought to act as a very efficient confinement for water molecules.

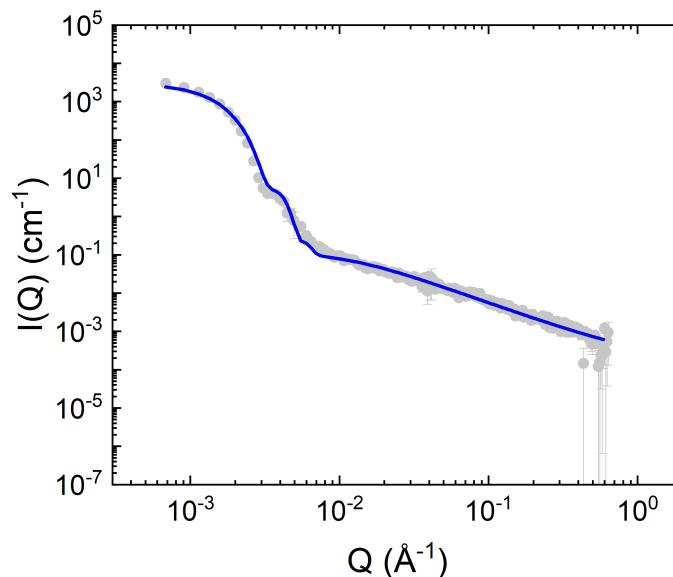


FIG. S4. Measured form factor of dilute samples of protiated PNIPAM microgels in  $D_2O$  (gray circles) and corresponding fits (blue line).

- 
- [S1] L. Tavagnacco, M. Zanatta, E. Buratti, B. Rosi, B. Frick, F. Natali, J. Ollivier, E. Chiessi, M. Bertoldo, E. Zaccarelli *et al.*, *Physical Review Research*, 2021, **3**, 013191.
  - [S2] E. Buratti, *et al.*, *manuscript in preparation*, 2024.
  - [S3] G. Del Monte, A. Ninarello, F. Camerin, L. Rovigatti, N. Gnan and E. Zaccarelli, *Soft Matter*, 2019, **15**, 8113–8128.
  - [S4] M. Stieger, J. S. Pedersen, P. Lindner and W. Richtering, *Langmuir*, 2004, **20**, 7283–7292.
  - [S5] J. E. Houston, L. Fruhner, A. de la Cotte, J. Rojo González, A. V. Petrunin, U. Gasser, R. Schweins, J. Allgaier, W. Richtering, A. Fernandez-Nieves *et al.*, *Science Advances*, 2022, **8**, eabn6129.